Contribution from the Departments of Chemistry, University of Missouri—Rolla, Rolla, Missouri 65401, and University of Missouri—Columbia, Columbia, Missouri 65201, Dipartimento di Chimica Inorganica Metallorganica ed Analitica, Università di Padova, I-35131 Padova, Italy, and Centro di Ricerca sui Biopolimeri del CNR, I-35131 Padova, Italy

Single-Crystal X-ray and Mössbauer Effect Study of Iron(III) Crown Ether Complexes

Umberto Russo, Giovanni Valle, Gary J. Long,* and Elmer O. Schlemper

Received July 17, 1986

An investigation of the complexes formed between iron and crown ethers has led to the isolation of the microcrystalline complexes $(FeCl_4)_3[Fe(H_2O)_6](18\text{-}6)_3(H_2O)_2$, $H[FeBr_4(18\text{-}6)(H_2O)_2]$, $FeCl_3(15\text{-}5)(H_2O)_2$, and $FeBr_3(15\text{-}5)(H_2O)_2$ and to single crystals of $H[FeBr_4(18\text{-}6)_2(H_2O)_{2.3}]$, where (18-6) represents the cyclic 18-crown-6 ether and (15-5) represents the cyclic 15-crown-5 ether. The structure of the single crystals has been determined at 295 and 120 K and reveals a cubic crystal with space group *Fd*3, No. 203, a *Z* of 8, and a lattice parameter *a* of 20.600 (4) Å at 295 K and 20.475 (1) Å at 120 K. The structure contains tetrahedral $FeBr_4$ anions that have no bonding interaction with the 18-crown-6 ether. The crown ether, which serves as a dielectric medium to separate the anions, has the expected D_{3d} symmetry and a longer than typical carbon–carbon bond. The Mössbauer effect spectral and magnetic properties of all the complexes reveal high-spin iron(III) in either a tetrahedral or octahedral coordination environment. Only one iron environment is found in all the complexes except $(FeCl_3)_4(18\text{-}6)_3(H_2O)_8$, which has two different iron(III) sites in the ratio of 3:1, that corresponded to tetrahedral and octahedral sites, respectively, and may be formulated as $(FeCl_4)_3[Fe(H_2O)_6](18\text{-}6)_3(H_2O)_2$. This complex undergoes facile decomposition induced by either heat or ultraviolet radiation in a variety of atmospheres to yield methane, carbon monoxide, and mixtures of hydrates of iron(II) chloride. The decomposition, under a variety of conditions, has been monitored by the Mössbauer effect of the iron-containing products. Similar results are obtained for the $H[FeBr_4(18\text{-}6)(H_2O)_2]$ complex.

Introduction

The first-row transition metals form a variety of complexes with different crown ethers, which normally act as second sphere ligands.[1] The linkage between the crown ether and the metal center is usually provided by one or more water molecules. These water molecules are directly coordinated to the metal and hydrogen-bonded to the oxygens of the crown ether. The crystal structures of the adducts between 18-crown-6 and manganese(II), cobalt(II), and nickel(II) have been reported.[2] These metals adopt an octahedral coordination sphere of six water molecules for the first two cations and of two chloride ions and four water molecules for the nickel(II) compound. These water molecules are hydrogen-bonded to the ethereal crown ether oxygens with hydrogen-bond distances ranging from 2.73 to 2.91 Å. As a consequence of this network of hydrogen bonds, the octahedral coordination around the metals is slightly distorted with angles ranging from 83.m to 98.4°.

A direct bond between the metal and the crown ether oxygens has been reported[3] only in complexes with the smaller 15-crown-5 and 12-crown-4 ethers. In these compounds the metal coordination sphere is normally completed by the anion or by water molecules. Cobalt(II) nitrate forms two complexes[3] in which the metal is seven-coordinate and bonded to all the oxygens of the 15-crown-5 or the 12-crown-4 and to two water molecules or to one bidentate and one monodentate nitrate ligand, respectively. In a similar way, copper(II) chloride forms a seven-coordinate complex with a substituted 15-crown-5 ether[4] and a six-coordinate complex with the 12-crown-4 ether.[5] In both cases, the two chloride ions complete the metal coordination sphere. Manganese(II) forms a complex[6] in which the metal is bonded exclusively to the oxygens of the crown ether. In this case the two 12-crown-4 ether molecules are staggered about the manganese(II), forming a regular square-antiprismatic eight-coordinate complex.

To date, only one example of a complex of known structure[7] between a crown-ether and iron has been published. In this complex of iron(II) with two 12-crown-4 ether ligands, the ligands form a "sandwich-like" configuration around the central iron atom. Recently there has been a report of an iron(III) chloride complex with a benzo-15-crown-5 ether and some related substituted crown ethers, but no structural details were provided.[8] The purpose of this paper is to present our results on the synthesis of several iron(III) complexes with two different crown ethers, to report the crystal structure of one such complex, and to describe their unusual oxidation–reduction behavior.

Experimental Section

Synthetic Preparations. Several reactions between iron(II) salts and 18-crown-6 ether dissolved in triethyl orthoformate or methanol produced either oily materials that could not be transformed into crystalline solids or highly unstable products that clearly decomposed even in an inert atmosphere. As a result, no stable iron(II) complexes could be obtained. The iron(III) complexes were prepared according to the following procedures. Iron(III) halide (2.0 mmol) was dissolved in the minimum amount of methanol, and the resultant solution was filtered into a methanolic solution of the crown ether (2.0 mmol). The volume of the resulting solution was decreased by solvent evaporation, and a solid yellow chloride complex or a deep red bromide complex was obtained by adding diethyl ether in a large excess, which resulted in the immediate precipitation of a fine microcrystalline powder. The solids were washed with a mixture of methanol and diethyl ether and dried under vacuum. All the preparative work was carried out in the air at room temperature and in the *absence* of fluorescent lighting. The experimental and calculated elemental analyses are given in Table I.[9] In the case of the reaction of 18-crown-6 with iron(III) bromide, the slow evaporation of the methanol, rather than the rapid precipitation with diethyl ether, led to the formation, over a period of days, of a different complex, $H[FeBr_4(18\text{-}6)_2(H_2O)_{2.3}]$, whose single crystal structure is reported herein. This slow pre-

* To whom correspondence should be addressed at the University of Missouri—Rolla.

(1) Su, A. C. L.; Weiher, J. F. *Inorg. Chem.* **1968**, *7*, 176–177. Knöchel, A.; Klimes, J.; Oehler, J.; Rudolph, G. *Inorg. Nucl. Chem. Lett.* **1975**, *11*, 787. Farago, M. E. *Inorg. Chim. Acta* **1977**, *25*, 71–76. DeVos, D.; VanDaalen, J.; Knegt, A. C.; VanHeyningen, T. C.; Otto, L. P.; Vonk, M. W.; Wijsman, A. J. M.; Driessen, W. L. *J. Inorg. Nucl. Chem.* **1975**, *37*, 1319–1320.
(2) Knöchel, A.; Kopf, J.; Oehler, J.; Rudolph, G. *Inorg. Nucl. Chem. Lett.* **1978**, *14*, 61. Vance, T. B., Jr.; Holt, E. M.; Pierpont, C. G.; Holt, S. L. *Acta Crystaallogr., Sect. B: Struct. Crystallogr. Cryst. Chem.* **1980**, *B36*, 150–153. Vance, T. B., Jr.; Holt, E. M.; Varie, D. L.; Holt, S. L. *Acta Crystallogr., Sect. B: Struct. Crystallogr. Cryst. Chem.* **1980**, *B36*, 153–155. Jarrin, J.; Dawans, F.; Robert, F.; Jeannin, Y. *Polyhedron* **1982**, *1*, 409–412.
(3) Holt, E. M.; Alcock, N. W.; Hendrixson, R. R.; Malpass, G. D., Jr.; Ghirardelli, R. G.; Palmer, R. A. *Acta Crystallogr., Sect. B: Struct. Crystallogr. Cryst. Chem.* **1981**, *B37*, 1080–1085.
(4) Sakurai, T.; Kobayashi, K.; Tsuboyama, S.; Kohno, Y.; Azuma, N.; Ishizu, K. *Acta Crystallogr., Sect. C: Cryst. Struct. Commun.* **1983**, *C39*, 206–208.
(5) van Remoortere, F. P.; Boer, F. P; Steiner, E. C. *Acta Crystallogr., Sect. B: Struct. Crystallogr. Cryst. Chem.* **1975**, *B31*, 1420–1426.
(6) Hughes, B. B.; Haltiwanger, R. C.; Pierpont, C. G.; Hampton, M.; Blackmer, G. L. *Inorg. Chem.* **1980**, *19*, 1801–1803.
(7) Meier, K.; Rihs, G. *Angew. Chem., Int. Ed. Engl.* **1985**, *24*, 858–859.
(8) Abrahim, J.; Marji, D. *Inorg. Chim. Acta* **1985**, *101*, L23–24. Marji, D.; Abrahim, J. *Inorg. Chim. Acta* **1985**, *105*, L3–4.
(9) See supplementary material.

0020-1669/87/1326-0665$01.50/0

Table II. X-ray Crystallographic Data and Structure Refinement

	295 K	120 K
chem formula	$H[FeBr_4(C_{12}H_{24}O_6)_2(H_2O)_{2.9}]$	$H[FeBr_4(C_{12}H_{24}O_6)_2(H_2O)_{2.3}]$
cryst syst	cubic	cubic
space group (no.)	*Fd*3 (203)	*Fd*3 (203)
lattice params		
a, Å	20.600 (4)	20.475 (1)
V, Å^3	8742	8583.6
Z	8	8
F(000)	3872	3821.6
density (calcd), g/cm^3	1.455	1.465
density (measd), g/cm^3	1.55	
color	dark red	dark red
cryst habit	cubic	cubic
Mo Kα wavelength, Å	0.7107	0.7107
beam monochromator	graphite	graphite
cryst dimens, mm	0.15 × 0.15 × 0.15	0.23 × 0.33 × 0.33
abs coeff, cm^{-1}	39.5	40.883
transmission factors		
min		69.28
av		82.11
max		99.94
abs corr	none	none
diffractometer	Philips PW1100	Enraf-Nonius CAD4
2θ range, deg	4–50	4–60
total no. of reflcns collected (*R*)	2109 (0.02)	1626
no. of unique reflcns collected	656	392
no. of refined variables	40	73
no. of reflcns used in refinement	284 (above 4σ)	287 (above 2σ)
soln of structure	Patterson, Fourier	direct, Fourier
computer program	SHELX-76	CAD4 SDP
final *R* factor	0.053	0.032
final weighted *R* factor	0.053	0.042
minimizn function	$w = 1$	$\sum w(\|F_o\| - \|F_c\|)^2$

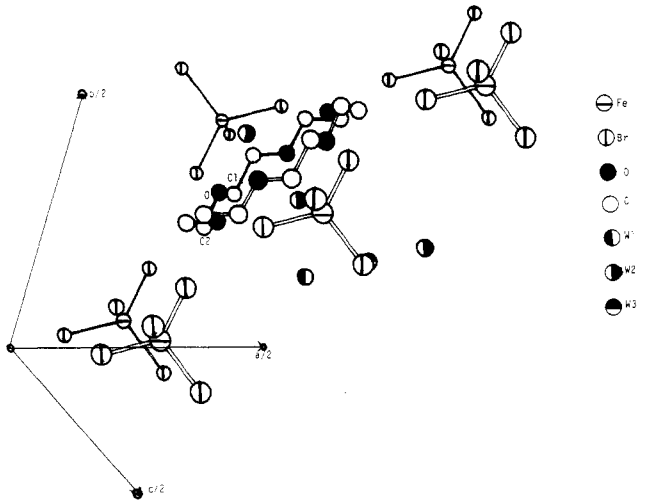

Figure 1. Perspective view of $H[FeBr_4(18\text{-}6)_2(H_2O)_{2.3}]$ showing one crown ether in the $FeBr_4$ anion network.

cipitation from methanolic solutions containing various iron(III) bromide to (18-6) crown ether ratios always led to the formation of $H[FeBr_4(18\text{-}6)_2(H_2O)_n]$, whereas rapid precipitation with diethyl ether always yielded $H[FeBr_4(18\text{-}6)(H_2O)_2]$.

Physical Measurements. The magnetic measurements were made on a Faraday balance, which utilized a Janis Supervaritemp helium cryostat and a Lake Shore Cryotronics temperature controller and was calibrated with $HgCo(SCN)_4$. The infrared spectra were obtained on a Perkin-Elmer 521 spectrometer by using KBr pellets. The differential thermal gravimetric results were obtained on a Mettler differential thermal analyzer. The Mössbauer effect spectra were obtained at 78 K on a conventional constant-acceleration spectrometer, which utilized a room-temperature rhodium matrix cobalt-57 source and was calibrated at room temperature with natural α-iron foil. The spectra were fit to Lorentzian line shapes by using least-squares computer minimization techniques. A Hanova low-pressure 450-W lamp was used for the ultraviolet irradiation experiments.

Crystallographic Data and Structure Refinement. The crystal structure of $H[FeBr_4(18\text{-}6)_2(H_2O)_n]$ has been determined at 295 and 120 K by using crystals obtained in different preparations. The details of the crystallographic parameters and the structural refinement procedures are listed in Table II. The space group determination was unambiguous, and standard scattering factors[10] were used in the refinement. The low-temperature structure was undertaken in order to improve the ratio of re-

Table V. Atomic Positional Parameters, Multiplicities, and Isotropic Equivalent Thermal Parameters Obtained for $H[FeBr_4(18\text{-}6)_2(H_2O)_{2.3}]$ at 120 K

atom	*x*	*y*	*z*	mult	*B*, Å^2
Fe	0.12500	0.12500	0.12500	0.0833	2.48 (6)
Br	0.05890 (3)	0.05890 (3)	0.05890 (3)	0.3333	3.062 (7)
O(1)	0.2188 (3)	0.3989 (3)	0.1607 (3)	1.0000	5.2 (1)
C(1)	0.2726 (4)	0.3774 (5)	0.1244 (4)	1.0000	5.2 (2)
C(2)	0.1862 (5)	0.3478 (4)	0.1933 (4)	1.0000	5.7 (2)
OW(1)	0.319 (4)	0.319 (4)	0.319 (4)	0.0960	14 (1)
OW(2)	0.459 (3)	0.459 (3)	0.459 (3)	0.1370	10.3 (9)
OW(3)	0.396 (3)	0.396 (3)	0.396 (3)	0.0800	11 (2)

Table X. Structural Parameters for $H[FeBr_4(18\text{-}6)_2(H_2O)_n]$

	bond dist, Å	
	295 K	120 K
Fe–Br	2.333 (2)	2.3441 (4)
O(1)–C(1)	1.40 (2)	1.401 (9)
O(1)–C(2)	1.39 (2)	1.410 (8)
C(1)–C(2)	1.54 (2)	1.49 (1)
O(1)–OW(2)	3.10, 3.31	3.08, 3.29
OW(1)–OW(1)	2.87	3.252
OW(1)–OW(2)	2.90	2.978
OW(1)–OW(3)		2.725
OW(2)–OW(2)	2.99	2.915
OW(2)–OW(3)		3.294
	bond angle, deg	
	295 K	120 K
Br–Fe–Br	109.47	109.47
O(1)–C(1)–C(2)	106 (1)	107.9 (7)
O(1)–C(2)–C(1)	109 (1)	109.3 (8)
C(1)–O(1)–C(2)	111 (1)	112.9 (6)

(10) *International Tables for X-ray Crystallography*; Kynoch: Birmingham, England, 1969; Vol. 4, p 99.

Table XI. Mössbauer Effect Spectral Parameters[a]

compd	conditions[b]	δ	ΔE_Q	Γ	% A	assigment
$(FeCl_4)_3[Fe(H_2O)_6](18\text{-}6)_3(H_2O)$	pure	0.30	0.09	0.46	75[c]	site A, $FeCl_4^-$
		0.49	0.88	0.89	25[c]	site B, octahedral iron(III)
	100 °C, air	0.30	0.18	0.29	46	site A
		0.46	0.81	0.50	36	site B
		1.32	3.03	0.30	18	high-spin octahedral iron(II)
	100 °C, vacuum	0.31	0.22	0.33	40	site A
		0.48	0.77	0.49	22	site B
		0.62	1.65	0.31	21	tetrahedral iron(II)
		1.29	3.19	0.41	17	high-spin octahedral iron(II)
	100 °C, nitrogen	0.31	0.24	0.36	43	site A
		0.51	0.65	0.49	13	site B
		0.61	1.67	0.35	38	tetrahedral iron(II)
		1.22	3.32	0.44	6	high-spin octahedral iron(II)
	140 °C, nitrogen	0.31	0.20	0.36	56	site A
		1.35	3.54	0.30	44	high-spin octahedral iron(II)
	190 °C, nitrogen	0.32	0.17	0.32	24	site A
		1.23	1.16	0.36	18	high-spin octahedral iron(II)
		1.14	2.24	0.68	33	high-spin octahedral iron(II)
		1.32	3.49	0.34	25	high-spin octahedral iron(II)
	UV, nitrogen	0.31	0.17	0.51	53	site A
		0.42	0.88	0.76	40	site B
		1.33	3.17	0.32	7	high-spin octahedral iron(II)
	UV, vacuum	0.30	0.28	0.57	17	site A
		0.50	0.89	1.10	12	site B
		1.29	2.64	0.27	61	high-spin octahedral iron(II)
		1.32	3.33	0.26	10	high-spin octahedral iron(II)
	UV, air	0.32	0.19	0.31	45	site A
		0.50	0.74	0.52	18	site B
		1.19	2.58	0.27	8	high-spin octahedral iron(II)
		1.29	3.16	0.45	29	high-spin octahedral iron(II)
$H[FeBr_4(18\text{-}6)_2(H_2O)_{2.3}]$	pure	0.32	0.12	0.31	100	$FeBr_4^-$
$H[FeBr_4(18\text{-}6)(H_2O)_2]$	pure	0.34	0.18	0.30	100	$FeBr_4^-$
	100 °C, air	0.35	0.16	0.28	82	$FeBr_4^-$
		1.33	2.97	0.36	18	high-spin octahedral iron(II)
	100 °C, vacuum	0.34	0.21	0.28	25	$FeBr_4^-$
		0.45	0.88	0.57	61	high-spin iron(III)
		1.33	3.20	0.33	14	high-spin octahedral iron(II)
	100 °C, nitrogen	0.30	0.22	0.37	67	$FeBr_4^-$
		1.32	3.83	0.32	33	high-spin octahedral iron(II)
	250 °C, nitrogen	1.18	0.87	0.36	100	high-spin octahedral iron(II)
$FeCl_3(15\text{-}5)(H_2O)_2$		0.28	0.11	0.63	100	
$FeBr_3(15\text{-}5)(H_2O)_2$		0.22	0.20	0.28	100	

[a] All data in mm/s obtained at 78 K relative to room-temperature α-iron foil. [b] The temperature and atmosphere for thermolysis or ultraviolet irradiation. [c] Variable constrained to the value given.

finement reflections to refined variables, in order to better determine the hydrogen-bonding network, and in an attempt to locate the hydrogen ion required for charge neutrality. The two structures have slightly different water content and a slightly different distribution of the water on the crystallographic sites. The resulting crystal structure is illustrated in Figure 1 for the results obtained at 120 K, and observed structure factors are given[9] in Tables III and IV. The final positional parameters obtained at 120 K are given in Table V, and those obtained at 295 K are given[9] in Table VI. At 120 K the crown ether and bromine were refined with anisotropic thermal parameters, and all temperature factors and thermal vibration amplitudes are given[9] in Tables VII and VIII. The temperature factors obtained at 295 K are given[9] in Table IX. The bond lengths and angles are given in Table X.

Results and Discussion

The facile decomposition of the product obtained in the reaction between iron(II) salts and the 18-crown-6 ether, even under an inert atmosphere, may be attributed to the oxidation of the iron(II) by the peroxides formed by and contained within the crown ether. The Mössbauer spectrum of the product of the preliminary reaction between iron(III) chloride and the 18-crown-6 ether in methanol showed the presence of two overlapping quadrupole doublets due to two different high-spin iron(III) ions and a third quadrupole doublet which was attributed to an unexpected iron(II) species. For different preparations the ratio of the areas of these three quadrupole doublets varied, as did the elemental analyses. Iron(III) reduction by the reactants has been ruled out, and the only two factors that might be responsible for the reduction are heat and light. The reaction, when carried out at room temperature in the dark, yielded a pure iron(III) compound. Subsequent experiments indicated that both heat and ultraviolet radiation from the fluorescent lights were responsible for the reduction of iron(III). This discovery permitted the preparation of the series of iron(III) complexes with crown ethers listed in Table XI.

The infrared spectrum of $(FeCl_4)_3[Fe(H_2O)_6](18\text{-}6)_3(H_2O)_2$ is nearly identical with that of the bromide complex. The only difference is the presence of the chloride spectrum of a band at 376 cm^{-1}, which may be attributed to the asymmetric ν(Fe–Cl) stretch in the tetrahedral $[FeCl_4]$ monoanion, and a band at 345 cm^{-1}, which may be attributed to the ν(Fe–O) stretch in the $[Fe(H_2O)_6]^{3+}$ anion. In $H[FeBr_4(18\text{-}6)_2(H_2O)_{2.3}]$ the asymmetric ν(Fe–Br) stretch of the tetrahedral monoanions occurs at 285 cm^{-1} whereas in $H[FeBr_4(18\text{-}6)(H_2O)_2]$ this band occurs at 288 cm^{-1}. In $FeCl_3(15\text{-}5)(H_2O)_2$ and $FeBr_3(15\text{-}5)(H_2O)_2$ the analogous bands occur at 368 and 289 cm^{-1}. The ν(O–H) band of the water molecules is found at 3420 cm^{-1} as a very broad absorption, which seems to indicate the presence of weak hydrogen bonds. In the presence of the strong water–crown ether hydrogen bonds found[11] in $(H_3O)(18\text{-crown-}6)(ClO_4)$, this band is shifted to 2950 cm^{-1}, where it overlaps with the ν(CH) absorption. The β(COC) band

(11) Chênevert, R.; Rodigue, A.; Beauchesne, P.; Savoie, R. *Can. J. Chem.* **1984**, *62*, 2293–2298.

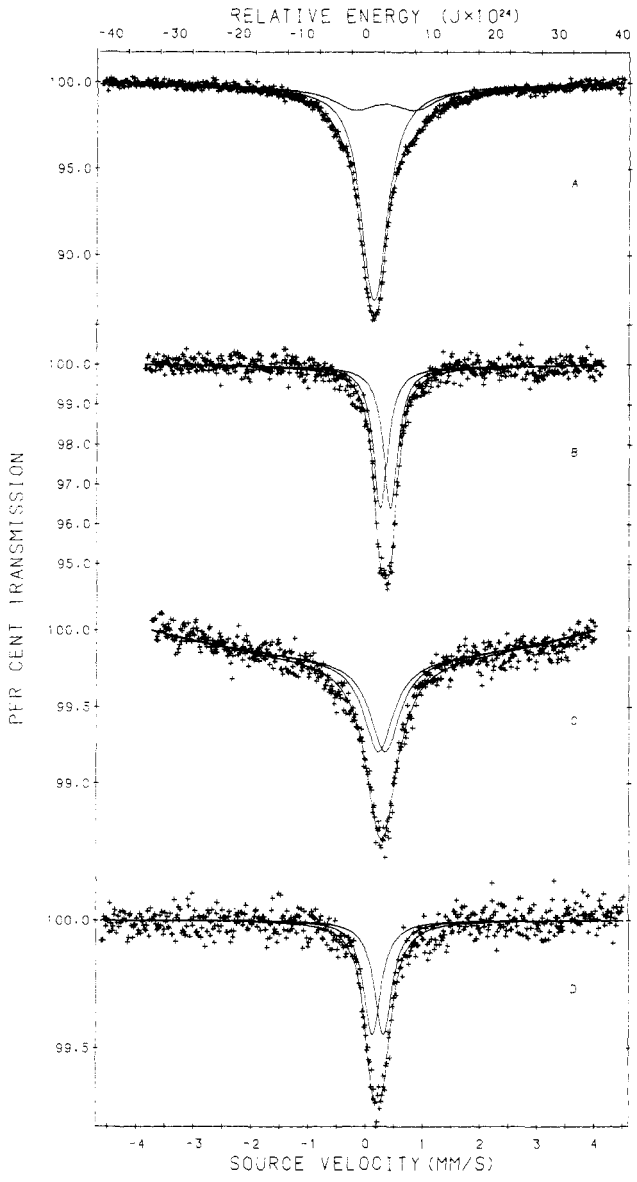

Figure 2. Mössbauer spectra (78 K) of $(FeCl_4)_3[Fe(H_2O)_6](18\text{-}6)_3(H_2O)_2$ (A), $H[FeBr_4(18\text{-}6)(H_2O)_2]$ (B), $FeCl_3(15\text{-}5)(H_2O)_2$ (C), and $FeBr_3(15\text{-}5)(H_2O)_2$ (D).

in the iron(III) complexes is only slightly affected by the hydrogen bonding and is found at 1105 cm^{-1} in all cases. The two bands at 830 and 960 cm^{-1}, which are unsplit in the potassium crown ether complex,[5,12] remain unchanged in these compounds. Hence, it appears the crown ether maintains its D_{3d} geometry. Some of these features, such as the low-frequency bands and the broad ν(OH) band at 3420 cm^{-1}, are maintained in the 15-crown-5 complexes. The band at 960 cm^{-1} is now split and appears at 940 and 965 cm^{-1}, while the intensities of the two peaks at 830 and 858 cm^{-1} are reversed upon complex formation. This may be due to the lowering of the crown ether symmetry by the formation of stronger hydrogen bonds.

The Mössbauer spectrum of the (18-6) iron chloride complex, illustrated in Figure 2A, shows the presence of two superimposed quadrupole doublets due to two different high-spin iron(III) ions, A and B, respectively, with an area ratio of 3:1. The spectral parameters for these two sites, as given in Table XI, indicate that, almost certainly, three of the four iron(III) ions are present in the form of $FeCl_4$ monoanions, which have virtually perfect tetrahedral symmetry as indicated by the small observed quadrupole splitting of 0.09 mm/s. The isomer shift of 0.30 mm/s is very characteristic[13] of this anion. The remaining iron(III) ion,

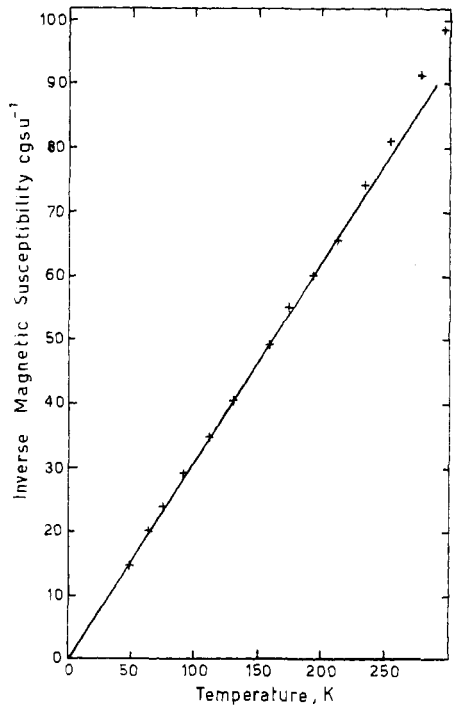

Figure 3. Temperature dependence of the inverse magnetic susceptibility of $(FeCl_4)_3[Fe(H_2O)_6](18\text{-}6)_3(H_2O)_2$.

with a larger isomer shift and quadrupole splitting, probably has a slightly distorted octahedral coordination environment made up of water molecules and perhaps a crown ether oxygen. Thus we propose the $(FeCl_4)_3[Fe(H_2O)_6](18\text{-}6)_3(H_2O)_2$ stoichiometry for this material. Unfortunately, all attempts to date to isolate single crystals of this material have failed. Repeated preparations do, however, lead to virtually identical elemental compositions and to exactly the same Mössbauer spectra as that shown in Figure 2A.

The Mössbauer spectra of the other complexes, as illustrated in Figure 2, show the presence of a single quadrupole doublet with a positive isomer shift and a very small quadrupole splitting in each case. The Mössbauer spectral parameters for these compounds are given in Table XI and are typical of high-spin iron(III) in a tetrahedral coordination geometry.[13] The room-temperature magnetic moments, given[9] in Table XII, agree with the high-spin nature of these products. The results for $(FeCl_4)_3[Fe(H_2O)_6](18\text{-}6)_3(H_2O)_2$, as a function of temperature, are shown in Figure 3. The observed moments are significantly smaller than the 5.92 μ_B value expected for isolated iron(III) ions, but the inverse susceptibility data extrapolate to 0 K, an indication of little or no magnetic coupling within the complex. Apparently extensive delocalization of the electrons onto the ligands accounts for the reduced magnetic moment.

Single crystals of the iron(III) bromide adduct with the 18-crown-6 ether, suitable for X-ray analysis, were obtained by slow evaporation of the methanol solvent in air. The structure was refined for the formula $H[FeBr_4(18\text{-}6)_2(H_2O)_n]$, where n is 2.3 for the 120 K structure and 2.9 for the 295 K structure. The cationic charge is apparently carried by a proton, which may be delocalized in the crown ether cavity or associated with the water molecules and was not detected in the X-ray analysis. The compound consists of discrete tetrahedral $FeBr_4$ anions, two crown ether molecules, and three sites occupied by variable amounts of water. A network of hydrogen bonds, as illustrated in Figure 1, connects these three water sites among themselves and with the ethereal oxygens. No contact distances of less than 4.16 Å have been found between the $FeBr_4$ anions and the water molecules

(12) Fouassier, M.; Lassegues, J. C. *J. Chem. Phys.* **1978**, *75*, 865.

(13) Clausen, C. A., III; Good, M. L. *Mössbauer Eff. Methodol.* **1968**, *4*, 187–200.

(14) Dunitz, J. D.; Seiler, P. *Acta Crystallogr., Sect. B: Struct. Crystallogr. Cryst. Chem.* **1974**, *B30*, 2739–2741.

or the crown ether. Hence, only electrostatic interactions hold together the various parts of the solid-state structure.

The crown ether ring in $H[FeBr_4(18\text{-}6)_2(H_2O)_n]$ has D_{3d} symmetry as in most of its other complexes and in agreement with that found in the infrared spectrum of the complex. The C–C bond distances of 1.54 Å is significantly longer than the 1.47 Å average found in other transition-metal complexes[2] and the 1.51 Å value found in the free crown ether molecule. In contrast, the C–O bond distance of 1.40 Å is only slightly shorter than the 1.43 Å average value reported for the coordinated ligand and the 1.41 Å value of the free ligand. The C–O–C and O–C–C bond angles are very close to the expected values of 112 and 110°.

The crown ether molecules are located around the $FeBr_4$ anions in the direction of the Fe–Br bonds at iron to crown distances of 5.76 and 6.81 Å. They completely surround the charged $FeBr_4$ anions in such a way that they serve as a dielectric medium, which reduces the $FeBr_4$ interanionic repulsion. Along the (111) axis, above and below the iron atoms, the three water sites contain variable amounts of water, but always in such a way that the sites either above or below the iron centers are occupied. As expected, the Mössbauer spectral parameters for $H[FeBr_4(18\text{-}6)_2(H_2O)_{2.3}]$ are typical of the $FeBr_4$ monoanion.[13] Because the anion symmetry is exactly tetrahedral, one would expect a zero quadrupole splitting. Apparently, the asymmetric distribution of the water and crown ether molecules about the $FeBr_4$ anion produces a small lattice contribution to the electric field gradient at the iron site.

Several experiments have been carried out to study the effect of heat and of ultraviolet light on the reduction of iron(III) in some of these compounds. The results have been evaluated principally by Mössbauer spectroscopy. In every case the reaction conditions strongly affect the amount and composition of the reduced material and the iron(III) site that undergoes the predominant reduction.

Reactions of $(FeCl_4)_3[Fe(H_2O)_6](18\text{-}6)_3(H_2O)_2$. The effects of ultraviolet light and heat on the reduction of this compound have been studied in detail under different conditions. The reactions were carried out in the air, under vacuum, or under nitrogen in order to study the effect of oxygen and water on the yield of the reduction and on the composition of the product.

The behavior of the compound under ultraviolet radiation is strongly dependent on the reaction conditions, and the amount of reduced material ranged from 9 to 62%, as illustrated in the Mössbauer spectra shown in Figure 4. An inert atmosphere inhibits the reduction, and only about 9% of the iron(III) is reduced, most of which is the iron(III) in $[Fe(H_2O)_6]^{3+}$. The Mössbauer parameters of the reduced material (see Table XI) are very similar to those of $FeCl_2 \cdot 4H_2O$.[15] The reaction in air produces at least two different iron(II) components, which correspond to 38% of the total area. The Mössbauer parameters are typical of iron(II) chloride with one, two, or four water molecules in the coordination sphere. However, the main product is $FeCl_2 \cdot 4H_2O$, which accounts for about 76% of the reduced material. The irradiation under vacuum produces the largest amount (62%) of reduced iron(II). In this case, much of the iron(II) seems to derive from the tetrahedral iron(III) chloride anions. The Mössbauer spectrum indicates that the iron(II) is mainly present as two different compounds, probably about 20% $FeCl_2 \cdot 4H_2O$ and 80% $FeCl_2 \cdot 2H_2O$. The gaseous products of this vacuum irradiation, as detected by mass spectrometry, are roughly equal amounts of methane and carbon monoxide, and traces of carbon dioxide. No chlorine, hydrogen chloride, or water were found in the vapor. The lack of water in the gas phase is in agreement with the Mössbauer results. It should be noted that $FeCl_2 \cdot 4H_2O$ contains more water per iron than $(FeCl_4)_3[Fe(H_2O)_6](18\text{-}6)_3(H_2O)_2$ and hence the water availability may be the limiting factor in this reduction.

The effect of heat on the iron(III) reduction is even more surprising, as illustrated[9] in Figure 5, because, for instance, some iron(II) material is obtained simply by heating the sample even in the presence of oxygen. The inert-atmosphere differential

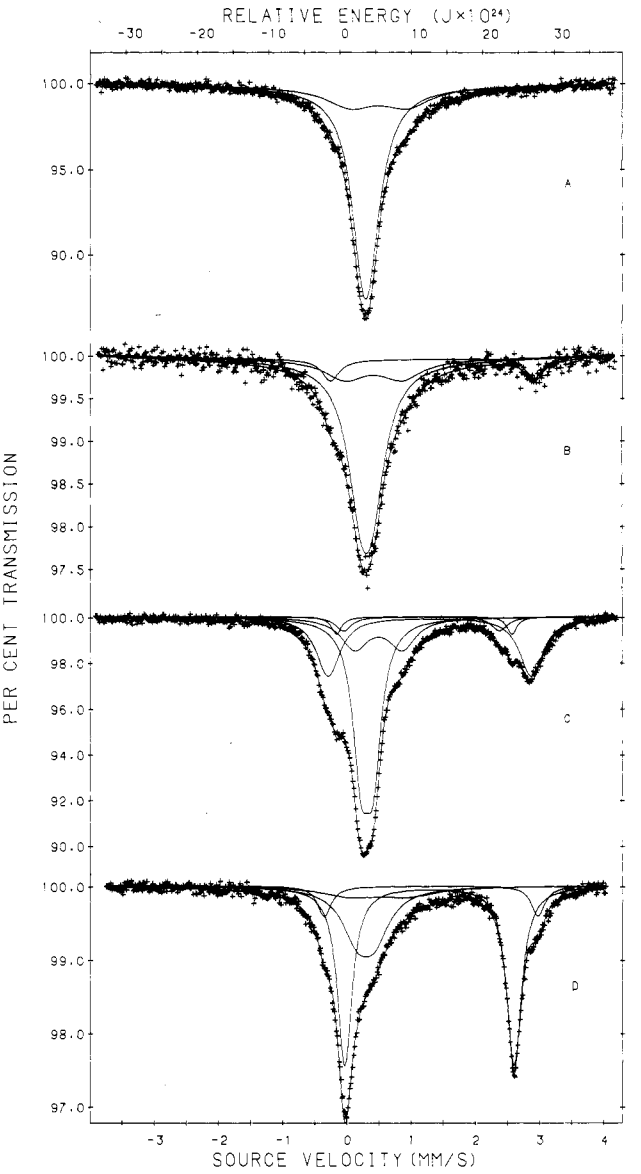

Figure 4. Mössbauer spectra (78 K) of pure $(FeCl_4)_3[Fe(H_2O)_6](18\text{-}6)_3(H_2O)_2$ (A) and its decomposition products when irradiated with ultraviolet radiation under nitrogen (B), in air (C), and under vacuum (D).

thermal gravimetric analysis of this complex, as illustrated in Figure 6, shows the presence of three, partly overlapping, reactions occurring at 70, 170, and 250 °C with a weight loss of about 6, 17, and 42%, respectively. None of these reactions correspond to the loss of any obvious component of the starting material. This points out that a complex decomposition reaction is taking place, even at the lowest temperature, rather than the simple loss of any molecular component. The Mössbauer spectra of the material, presented in Figure 5 and obtained after the first weight loss and before and after the second weight loss (at 100, 140, and 190 °C, respectively), show an increasing amount of reduced material and, under certain conditions, the appearance of a new species. The conditions under which the reduction is carried out strongly affect both the nature of the decomposition of the starting material and the amount and composition of the reduced products. Heating the sample in the air (see[9] Figure 7B) at 100 °C produces 18% of a single iron(II) species that mainly results from the decomposition of the iron(III) tetrachloro anions and is most likely $FeCl_2 \cdot 4H_2O$. If the sample is heated at 100 °C under vacuum (Figure 7C), the yield of the reduction is higher (about 38%) and a new intermediate species appears in large quantity, and is about 55% of the reduced material. Its Mössbauer parameters indicate that it may be a highly distorted tetrahedral iron(II) compound,

(15) Brunot, B. *J. Chem. Phys.* **1974**, *61*, 2360–2366.

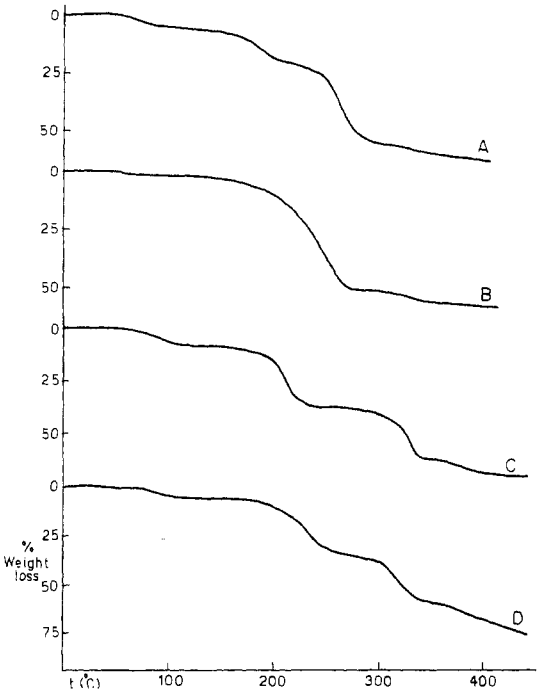

Figure 6. Thermal gravimetric plots obtained in an argon atmosphere for $(FeCl_4)_3[Fe(H_2O)_6](18\text{-}6)_3(H_2O)_2$ (A), $H[FeBr_4(18\text{-}6)(H_2O)_2]$ (B), $FeCl_3(15\text{-}5)(H_2O)_2$ (C), and $FeBr_3(15\text{-}5)(H_2O)_2$ (D).

whose production may be inhibited by the presence of oxygen, because it appears only when the reduction is carried out in the absence of air. It is interesting to note that this product never appears in the ultraviolet-induced reduction (see Figure 4), and so it seems probable that the two reactions follow different mechanistic pathways. A very similar Mössbauer spectrum (Figure 7D) is obtained when the material is decomposed under nitrogen. The amount of reduced iron is now increased slightly from 38 to 44%. The tetrahedral iron(II) species seems to be an unstable intermediate as it completely disappears at 140 °C, even before the second step of the decomposition, to form the octahedral $FeCl_2 \cdot 4H_2O$ species. In this temperature range, the $[Fe(H_2O)_6]^{3+}$ ion is apparently transformed into chloro-bridged iron(III) ions or into $FeCl_2 \cdot 4H_2O$. At this point the only species present in the material are tetrahedral iron(III) anions and $FeCl_2 \cdot 4H_2O$. The second step of the thermal decomposition shows a large increase in the reduced material (see Figure 5D), which now reached 76% of the total area. The two new quadrupole doublets in the Mössbauer spectrum may be attributed to iron(II) chloride, which is undergoing a progressive dehydration.[16] The tetrahydrate of iron(II) chloride now accounts for only 25% of the total area.

Reactions of $HFeBr_4(18\text{-}6)(H_2O)_2$. Similar experiments have been carried out on the iron(III) bromide complex with the 18-crown-6 ether. The differential thermal gravimetric analysis shown in Figure 6 indicates a two-step decomposition. In the first step, centered at ca. 60 °C, only a few percent of the weight of the starting material is lost. This is probably due to the loss of part of the water and to some reduction of iron(II) as indicated in Figure 8B. The second step, centered at ca. 200 °C, results in the loss of 47% of the starting material. The Mössbauer spectrum (Figure 8B,C) indicates that, concurrently with the first decomposition, a partial iron(III) reduction has taken place, with the consequent formation of a high-spin iron(II) species. It is interesting that heating the sample at 100 °C under vacuum produces a large amount of a second iron(III) species with a rather large quadrupole splitting. Heating the sample under nitrogen at 100 °C yields a spectrum similar to that shown in Figure 8D,

(16) Long, G. J. In *Mössbauer Spectroscopy*; Dickson, D. P. E., Berry, F. J., Eds.; Cambridge University Press: London, 1986; Chapter 3, p 70.

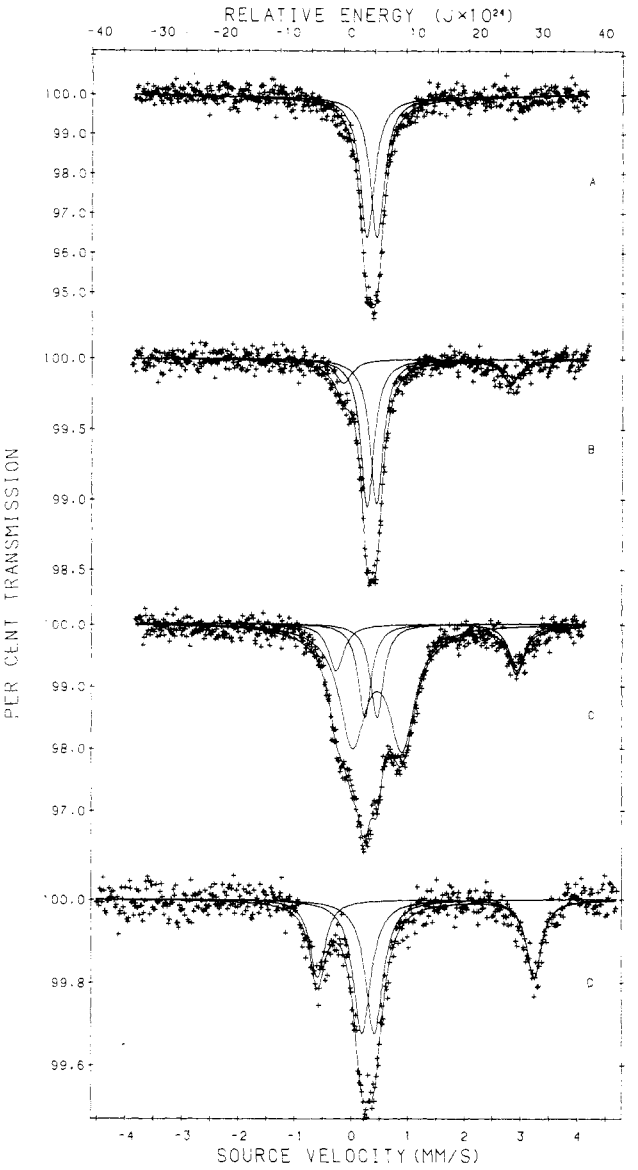

Figure 8. Mössbauer spectra (78 K) of pure $H[FeBr_4(18\text{-}6)(H_2O)_2]$ (A) and its decomposition products when heated at 100 °C in air (B), under vacuum (C), and under nitrogen (D).

whereas heating at 250 °C yields a quadrupole doublet typical of tetrahedral iron(II).

These unexpected reduction reactions induced by both heat and ultraviolet light explain the lack of previous reports in the literature dealing with these complexes. More work is currently in progress to understand more fully the mechanism of this reduction and the nature of the concurrent oxidation product.

Acknowledgment. We gratefully acknowledge the financial support of the Ministero della Pubblica Istruzione, Italy. We thank the donors of the Petroleum Research Fund, Administered by the American Chemical Society, and the National Science Foundation (Grant No. INT-8202403) for their financial support of this research. We thank Drs. R. K. Murmann, G. Bertrand, D. Wulfman, and G. Schade and D. E.Tharp and M. L. Buhl for their collaboration and helpful discussions during the course of this work.

Supplementary Material Available: Figures 5 and 7 (Mössbauer spectra of $(FeCl_4)_3[Fe(H_2O)_6](18\text{-}6)_3(H_2O)_2$ after decomposition under various conditions), Table I (analytical results), Table VI (atomic positional parameters at 295 K), Tables VII–IX (general temperature factors and thermal vibrations), and Table XII (magnetic susceptibility data) (8 pages); Tables III and IV (structure factors) (4 pages). Ordering information is given on any current masthead page.